Pramana – J. Phys., Vol. 39, No. 5, November 1992, pp. 547–557. © Printed in India.

A new polarization potential for heavy ion fusion spin distribution

A K MOHANTY, S K KATARIA and S V S SASTRY
Nuclear Physics Division, Bhabha Atomic Research Centre, Bombay 400085, India

MS received 10 March 1992

Abstract. The real part of the polarization potential which depends on both energy and angular momentum is calculated in a simple way using dispersion relation. A barrier penetration model (BPM) has been used to explain the fusion cross-section and compound nucleus spin distribution for $^{32}S + ^{64}Ni$ system in the energy range 50–75 MeV. It is also shown that the polarization potential which only depends on energy, is not adequate to give rise to correct spin distribution even after including any radial dependence. The proposed polarization potential with implicit E and l dependences is able to explain both fusion cross-section and average spin values.

Keywords. Fusion cross-section; compound nucleus spin distribution; barrier penetration model; polarization potential.

PACS Nos 25·70; 24·10

1. Introduction

The enhancement of fusion cross-sections and broadening of compound nucleus spin distribution of two heavy nuclei at energies around the coulomb barrier are quite well-known. A simple barrier penetration model (BPM) where the potential is a function of one parameter i.e. the distance between the two nuclei is not adequate to explain fusion cross-section at sub-barrier energies as well as the observed large spin values (Beckerman 1985, 1988; Steadman 1985; Steadman and Rhooder-Brown 1986; Halbert *et al* 1989; Vandenbosch *et al* 1986), even though it explains them correctly at much higher barrier energies. Several theoretical approaches have been developed in order to understand the reaction mechanism at near and sub-barrier energies. Modifications of the fusion potential by deformations (Wong 1973), coupling to inelastic excitations (Dasso *et al* 1983a, b), nucleon transfer (Broglia *et al* 1983), zero point motion (Esbensen 1981) and neck formation (Aguair *et al* 1985; Iwamoto and Harada 1987; Ramamurthy *et al* 1990), have been shown to yield substantial enhancements of sub-barrier fusion cross-sections. Therefore, sub-barrier fusion is an interesting process for probing the role of different degrees of freedom in quantum mechanical tunneling processes. A more stringent test of different models can be obtained by comparing not only the fusion cross-section but also the shape of the fusion spin distribution. Models which have different physical input can give rise to different spin distribution (Dasso *et al* 1989), as partial wave distribution for fusion is more sensitive to the detailed contents of the model than the cross-section and thus, the determination of the spin distribution provides much tighter constraints on the different theories of sub-barrier fusion enhancement. A detailed coupled channel calculation where the non-elastic channel, both inelastic and transfer channels are

treated explicitly have been more successful in explaining enhancement in fusion cross-section as well as giving rise to broad spin distribution. These channel couplings allow the ions to polarize each other as they come together. One way of representing this is through the introduction of distribution of barriers (Dasso *et al* 1983a, b), one or more of which will be lower than the uncoupled barrier height. Hence, it will enhance the penetration when the incident energy is close to, or below, the uncoupled barrier height. The channel couplings have little effect when the incident energy is appreciably higher than the channel barrier heights.

The importance of couplings between various channels is also seen in simple phenomenological model such as optical model analysis of elastic scattering data where it was found that the strength of the real and imaginary potential vary rapidly with energy (Lilley *et al* 1985; Fulton *et al* 1985; Baeza *et al* 1984). This class of phenomena popularly known as threshold anomaly is simply an expression of the effects of the coupling to the non-elastic channels and has the same origin as that of enhancement of sub-barrier fusion (Mahaux *et al* 1986a, b). The same results could be obtained in a simpler way by using an energy dependent barrier height in BPM calculations. In other words, the nuclear potential becomes energy dependent due to polarization effect and this real polarization potential $\Delta V(E)$ can be calculated from the imaginary part of the optical potential through dispersion relation (Nagarajan *et al* 1985). However, to make the spin distribution broad, the radial dependence of the polarization potential $\Delta V(E, r)$ should also be taken into account. It has been shown that (Satchler *et al* 1990; Satchler 1991; Kubo *et al* 1991), optical model analysis for fusion can give rise to different spin distribution depending on different radial shape of the imaginary fusion potential $W_f(r)$ which itself is composed of a short range bare term $W_{of}(r)$ and a long range polarization term $W_{pf}(r)$ responsible for peripheral absorption. It is also known that (Rhoades-Brown and Braun-Munzinger 1984) the results of optical model analysis can be reproduced by WKB penetration through the real potential provided the imaginary part is short-range and remains well inside the barrier. Due to the polarization component, the imaginary potential extends beyond the top of the barrier and fusion is initiated at larger radius near or even beyond the top of the barrier. As $W_f(r)$ extends into the barrier, full penetration is not required. Alternatively, penetration with the WKB calculation which deals with the full traversal of the barrier will underestimate the fusion probability as fusion also takes place under the barrier. However, the polarization correction to real potential $\Delta V(E)$ can be included in WKB calculation to enhance the transmission as the real potential becomes more attractive and inclusion of any radial dependence of $\Delta V(E, r)$ also can make the barrier thin giving rise to large $\langle l \rangle$ as well as broad spin distribution. In this paper we show that inclusion of r-dependence $\Delta V(E, r)$ is not adequate to give rise to correct spin distribution with BPM model unless the real polarization potential is allowed to vary with angular momentum l in addition to its dependence on energy E. In the present work, this E and l dependent real polarization potential is calculated in a simple way using dispersion relation.

2. Model

Fusion cross-section at a given energy E and for partial wave l is written as:

$$\sigma_f(l) = (\pi/k^2)(2l+1)\, T_l(E), \tag{1}$$

where k is the wave vector and T_l is the penetration probability of l-th partial wave. In a simple BPM model $T_l(E)$ can be written as the well known Hill-Wheeler expression:

$$T_l(E) = [1 + \exp(2\pi/\hbar\omega)(V_0 + E_R - E)]^{-1} \tag{2}$$

where

$$E_R = l(l+1)\hbar^2/(2\mu R_0^2)$$

V_0, R_0 and $\hbar\omega$ are S-wave barrier height, barrier position and barrier width. The total fusion cross-section is the sum over all partial waves:

$$\sigma_f(E) = \sum_l \sigma_l, \tag{3}$$

and the various moments of the spin distribution are defined as

$$\langle l^n \rangle = \frac{\sum l^n \cdot \sigma_l}{\sum \sigma_l}. \tag{4}$$

In energy-dependent BPM model the barrier height V_0 becomes energy dependent. Therefore, V_0 is replaced by an effective barrier height V_{eff} which has an energy independent part V_0 and an energy dependent part $\Delta V(E)$ such that

$$V_{\text{eff}}(E) = V_0 + \Delta V(E). \tag{5}$$

The energy dependent part $\Delta V(E)$ is related to the imaginary part of the optical potential required to explain the elastic scattering data through dispersion relation (Nagarajan *et al* 1985)

$$\Delta V(E) = \frac{P}{\pi} \int_{-\infty}^{\infty} \frac{W(r, E')}{(E' - E)} \mathrm{d}E'. \tag{6}$$

The dispersion integral for $\Delta V(E)$ involves knowledge of $W(E)$ at all energies. In general, it is difficult to know this, particularly its high energy behaviour. However, an analytic form of this integral in (6) can be obtained assuming a linear model of $W(E)$ which seems to be adequate in a limited energy interval. In this model, $W(E)$ falls to zero beyond E_a, and assumes a constant value after E_b and is linear in the region $E_a < E < E_b$. With these approximations (6) can be written as

$$\Delta V(E, r) = \lambda(r)[K_a \log|K_a| - K_b \log|K_b|] \tag{7}$$

where

$$K_a = (E - E_a)/(E_b - E_a) \text{ and } K_b = (E - E_b)/(E_b - E_a).$$

This function is symmetric around mean energy $(E_a + E_b)/2$ and becomes zero at E_a and E_b. The radial dependence of $\Delta V(E, r)$ is given by the factor $\lambda(r) = W_0(r)/\pi$ i.e. it has the same radial dependence as that of imaginary potential. In another approximation, $\lambda(r)$ is evaluated at the interaction radius where the polarization correction is maximum and is written as $\Delta V(E)$. Now (7) has three parameters $\lambda_0(\lambda(r)$ at $r = R_0)$, E_a and E_b. These parameters are obtained from imaginary potentials needed in elastic scattering analysis.

3. Calculations

We have chosen $^{32}S + ^{64}Ni$ system for which elastic scattering, (Stefanini *et al* 1987), fusion cross-section and average spin values (Dasgupta *et al* 1991, 1992) are available. In the present study, the polarization potential ΔV has been calculated in three different ways. The effective potential in (5) can be written as:

Case I $V_{\text{eff}} = V_0 + \Delta V(E, R_0)$
(ΔV depends on energy E and is evaluated at a fixed $r = R_0$)

Case II $V_{\text{eff}} = V_0 + \Delta V(E, l, R_0)$
(ΔV depends on both E and l and is evaluated at $r = R_0$)

Case III $V_{\text{eff}} = V_0 + \Delta V(E, r)$
(The radial dependence of ΔV is included)

Case I: From the analysis of Udagawa *et al* (1989) we choose $E_b = 60$ MeV, above which $W(E)$ remains constant and $E_a = 44$ MeV, beyond which $W(E)$ vanishes. The polarization potential has maximum value at around $E = 52$ MeV. To verify these parameters E_a and E_b and to find out the strength factor λ_0, the effective barrier height V_{eff} was obtained from the experimental fusion cross-sections at each energy using

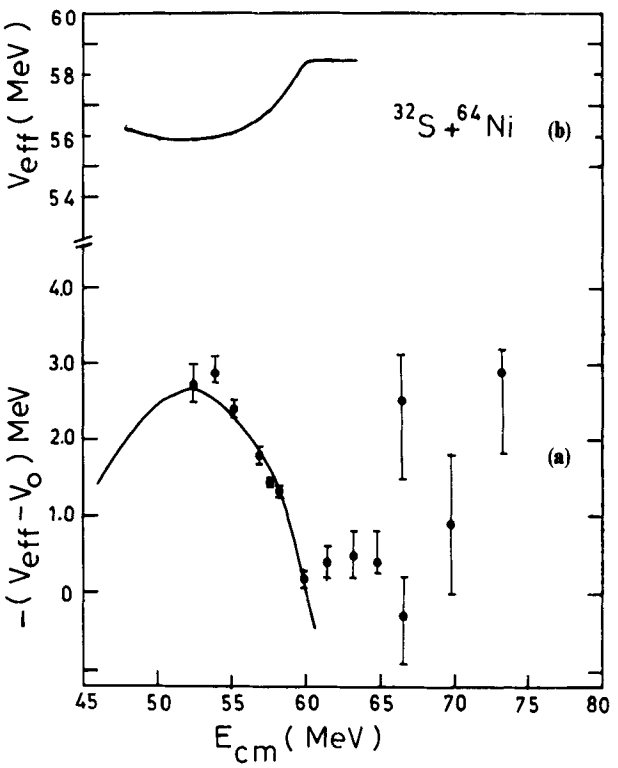

Figure 1. **(a)** $(V_{\text{eff}} - V_0)$ versus E_{cm} for $^{32}S + ^{64}Ni$ system. The solid dots with error bar derived inverting the experimental fusion cross-sections taken from Sefanini *et al* (1987) and Dasgupta *et al* (1991, 1992). The values of R_0, V_0 and $\hbar\omega$ used are 9·6 fm, 58·5 MeV and 4 MeV. **(b)** V_{eff} versus E_{cm} for $^{32}S + ^{64}Ni$ system.

(2) and (3). The value of R_0 and $\hbar\omega$ used are 9·6 fm and 4 MeV. Figure 1(a) shows the plot of $(V_{eff} - V_0)$ as a function of E_{cm}. V_0 is chosen to be 58·5 MeV, which fits the above barrier data. The above derived values of $(V_{eff} - V_0)$ can be parametrized using (7) with $E_a = 44$ MeV, $E_b = 60$ MeV and $\lambda_0 = 3{\cdot}82$ (see solid curve in figure 1(a)). Figure 1(b) shows the effective barrier height V_{eff} as a function of E_{cm}. As seen from this figure, the polarization correction $\Delta V(E)$ becomes positive after E_b, which increases effective potential V_{eff} beyond V_0. This positive polarisation correction arises as we have choosen a simple model for $W(E)$ which is constant for energies $E > E_b$. However, the data do not demand any further correction for energy greater than E_b, as a single barrier height V_0 can explain fusion cross-section well. Therefore, ΔV is set to zero for energy greater than E_b in these calculations.

Figure 2 shows (open circle) the plot of fusion cross-section for $^{32}S + {}^{64}Ni$ system at different energies with $\Delta V(E)$ given in figure 1. The dashed line is the result of energy independent BPM model with a constant barrier height V_0. The corresponding average spin values $\langle l \rangle$ (open circle and dashed line) are shown in figure 3. Using the energy dependent BPM model, even though the fusion cross-sections are reproduced well, it fails to reproduce the experimental $\langle l \rangle$ values. This discrepancy is seen more in the vicinity of the Coulomb barrier.

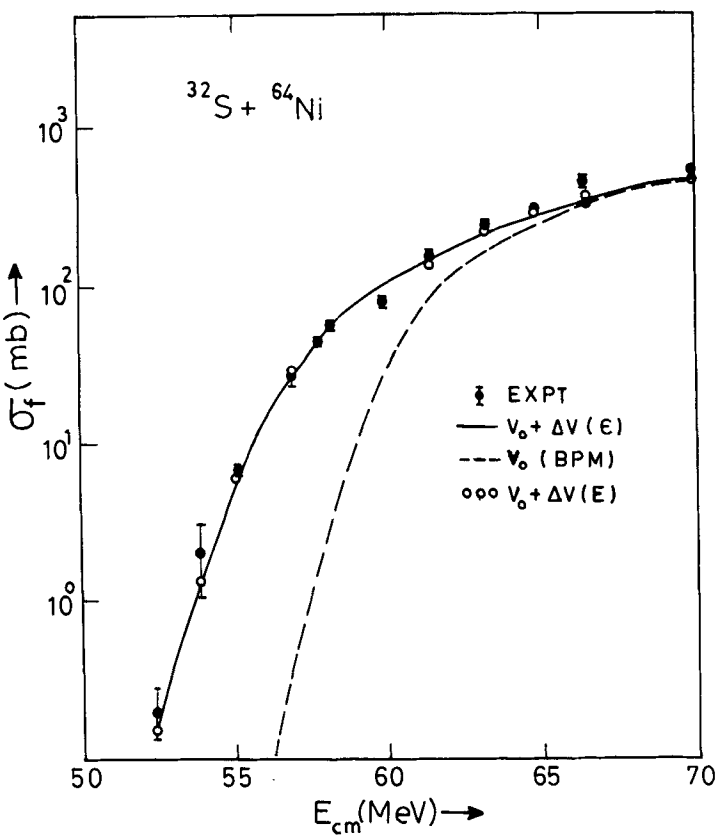

Figure 2. Fusion cross-sections versus E_{cm} for $^{32}S + {}^{64}Ni$ system. The solid line is the result of BPM using ΔV as a function of ε. The open circle is the result of BPM using ΔV as a function of E_{cm}. The dashed line is the result of energy independent BPM.

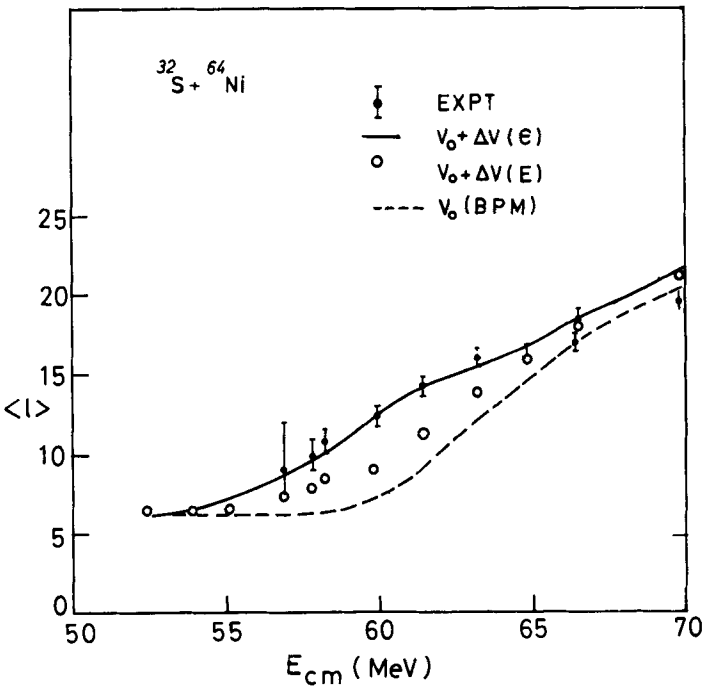

Figure 3. Average spin value $\langle l \rangle$ versus E_{cm}. The continuous curve, open circle and dashed line are the corresponding values of BPM as shown in figure 2.

Case II: In this case, fusion cross-sections are calculated using an E and l dependent polarization potential $\Delta V(E, l)$. This is carried out by making the optical imaginary potential E and l dependent. Following earlier studies (Mohanty *et al* 1990), the imaginary potential is written as a product of two factors $f(r)$ and $g(E, l)$ as:

$$W(E, r, l) = W_0 f(r) g(E, l), \tag{8}$$

where the radial part $f(r)$ has the form

$$f(r) = 1/[1 + \exp\{(r - R_0)/a_0\}]. \tag{9}$$

The energy and l dependent part has the form

$$g(E, l) = [1 + \exp\{(E_e - \varepsilon)/a_e\}]^{-1} \tag{10}$$

with

$$\varepsilon = E - \frac{l(l+1)\hbar^2}{2\mu R_0^2}. \tag{11}$$

Now the polarization potential will depend on both E and l as given by

$$\Delta V(E, l) = W_0 f(r) \frac{p}{\pi} \int_{-\infty}^{\infty} \frac{g(E', l)}{(E' - E)} \mathrm{d}E'. \tag{12}$$

From (10), it is obvious that

$$g(E, l) = g(\varepsilon, 0),$$

where ε is given by (11). Substituting $g(E,l)$ with $g(\varepsilon,0)$ in (12) and replacing the variable of integration from E' to ε, one can write

$$\Delta V(\varepsilon) = W_0 f(r) \frac{P}{\pi} \int_{-\infty}^{\infty} \frac{g(\varepsilon',0)}{(\varepsilon' - \varepsilon)} d\varepsilon'. \tag{13}$$

As seen from (13), the basic structure of (12) and (13) remains the same except that the variable of integration i.e. the energy variable E' is replaced by a new energy variable ε' as defined by (11). Therefore, one can use the same logarithmic form of (7) to calculate $\Delta V(\varepsilon)$, the only difference is that instead of calculating ΔV at energy E, one has to calculate ΔV at energy ε which depends on both E and l. As a result, the effective barrier height now depends on both l and E. At any high energy, there are some partial waves for which the barrier height is lower than V_0. Therefore, the potential V_0 has to be a little higher than the value used in earlier calculations. The values of $V_0 = 60{\cdot}4$ MeV and $\lambda_0 = 6{\cdot}52$ were chosen to reproduce the fusion data well

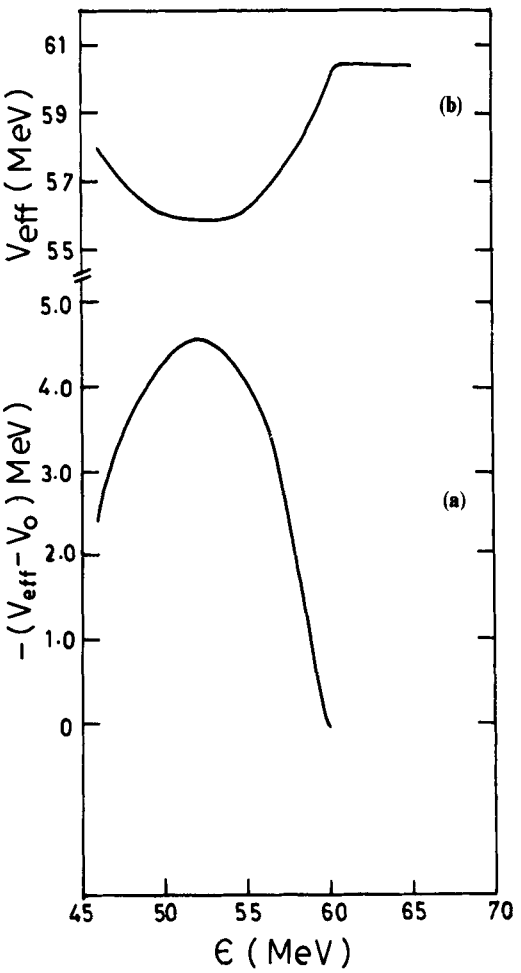

Figure 4(a, b). Same as figure 1(a, b). But here V_{eff} and ΔV depends on energy variable ε which depends on E and l.

(see solid line in figure 2). The values of E_a and E_b used are same as before i.e. 44 and 60 MeV. This value of V_0 is same as that obtained from a proximity type calculation with surface tension co-efficient $\gamma = 1{\cdot}25\ (1 - 2{\cdot}3I^2)$ (Blocki *et al* 1977). The corresponding value of $\langle l \rangle$ are shown in figure 3 as continuous line, which explains the experimental values rather well. The values of $\Delta V(\varepsilon)$ and $V_{\text{eff}}(\varepsilon)$ are also shown in figure 4 for comparision. Here also one sets the value of $\Delta V(\varepsilon)$ to zero for energy $\varepsilon > E_b$ and $\varepsilon < E_a$.

Case III: In cases I and II, ΔV is evaluated at a fixed radius R_0 i.e. ΔV is independent of r. In case III, calculations are carried out to see whether it is possible to explain observed large average spin values by including the radial dependence of the polarization potential along with only energy dependence $\Delta V(E, r)$, so that one need not introduce an extra l-dependence in polarization potential $\Delta V(E, r, l)$. For these calculations, a form factor $f(r)$ which has same radial dependence as that of imaginary optical potential is used to obtain $\Delta V(E, r) = \Delta V(E) \cdot f(r)$. Two extreme radial shapes i.e. (a) $f(r)$ having the Woods-Saxon form and (b) $f(r)$ having the surface peaked form, are studied.

$$\lambda(r) = \lambda_0 f(r), \tag{14}$$

where

(a) $f_w(r) = \lambda_0/\{1 + \exp(x)\}$ Woods-Saxon

(b) $f_s(r) = \lambda_0 \exp(x)/\{1 + \exp(x)\}^2$ Surface peaked

$$x = (r - R_0)/a_0.$$

With this radial dependence, the penetration factor using WKB approximation was calculated for the total potential $V(r) + \Delta V(E, r)$. The value of $r_0(R_0 = r_0 A^{1/3})$ and a_0 are 1·247 and 0·5 fm. The variation of ΔV with r as well as with E was studied to see whether it is possible to reproduce observed $\langle l \rangle$ values without invoking l-dependence of polarization potential. The radial dependence of polarization potential is shown in figures 5(a) and (b). Figure 5(a) shows only $\Delta V(E, r)$ and figure 5(b) shows the plot of total potential $V_T = V(r) + \Delta V(E, r)$ where $V(r)$ is the sum of nuclear and Coulomb potential. The nuclear potential is calculated from proximity parameters (Blocki *et al* 1977). The bare potential $V(r)$ (sum of nuclear and Coulomb potential) is shown by solid line in figure 5(b). When a constant correction $\Delta V(E)$ depending on energy is added, the total potential is scaled down by a constant amount $\Delta V(E)$ at each r (see dashed line). The dotted and the dashed dot lines are the result when ΔV has different r dependence. The dotted line is due to the radial dependence which has surface peaked form factor $f_s(r)$ and the dashed dot line is due to the radial dependence which has Woods-Saxon type form factor $f_w(r)$.

The results of spin distribution with different polarization potential ΔV are shown in figure 6 at two bombarding energies 56·9 MeV and 58·2 MeV. The dashed line is obtained with a constant polarization potential $\Delta V(E)$, the dashed dot line is with $\Delta V(E, r)$ where the radial dependence is Woods-Saxon type. The solid curve is the result of coupled channel calculations which includes 2^+ and 3^- states of ^{32}S and 2^+, 3^- and 4^+ states of ^{64}Ni and an additional coupling strength of 1 MeV at $Q = +5$ MeV arising due to particle transfer. The strength parameters and β values are taken from Stefanini *et al* (1987), Broglia *et al* (1985) and the simple code CCFUS

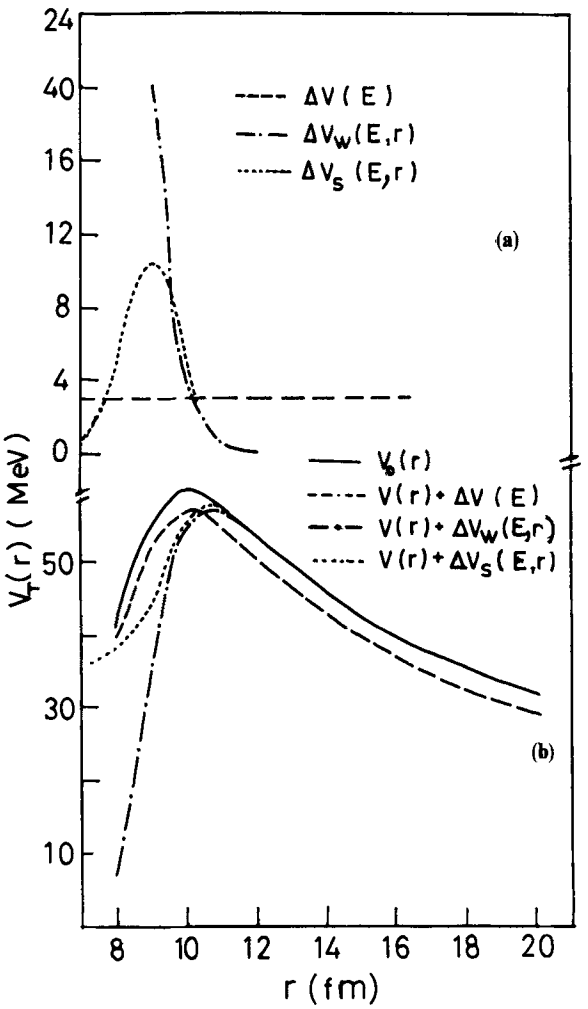

Figure 5(a). Polarization potential $\Delta V(E,r)$ versus r. The dashed line is for $\Delta V(E)$ which is independent of r. The dashed-dot line for $\Delta V(E,r)$ where the radial dependence is of Woods–Saxon type, while the dotted line is with the surface peaked radial dependence.
Figure 5(b). The total potential $V_T(r)$ versus r, with different polarization potential. The curves have same meaning as that of figure 5(a). The solid line is for the bare potential without any polarization correction.

(Broglia *et al* 1985; Dasso and Landowne 1987) was used for coupled channel calculations. The barrier heights were adjusted in each case to give same fusion cross-sections. As seen from figure, the spin distribution with and without radial dependence of ΔV (dashed dot and dashed curve) are slightly different; the inclusion of radial dependence giving slightly broader spin distribution than without radial dependence. However, both the results are much smaller than the coupled channel results which are quite close to the experimental values. As an example, the average $\langle l \rangle$ values for $E_{cm} = 58{\cdot}2$ MeV in the above three cases are 8·43, 8·8 and 11·2 where as the experimental value of $\langle l \rangle$ is $10{\cdot}8 \pm 0{\cdot}8$. In the figure we have not shown the result of spin distribution due to $\Delta V(E,r)$ with surface peaked form factor f_s, as it is almost similar to that of dashed-dot curve. For comparison, the spin distribution

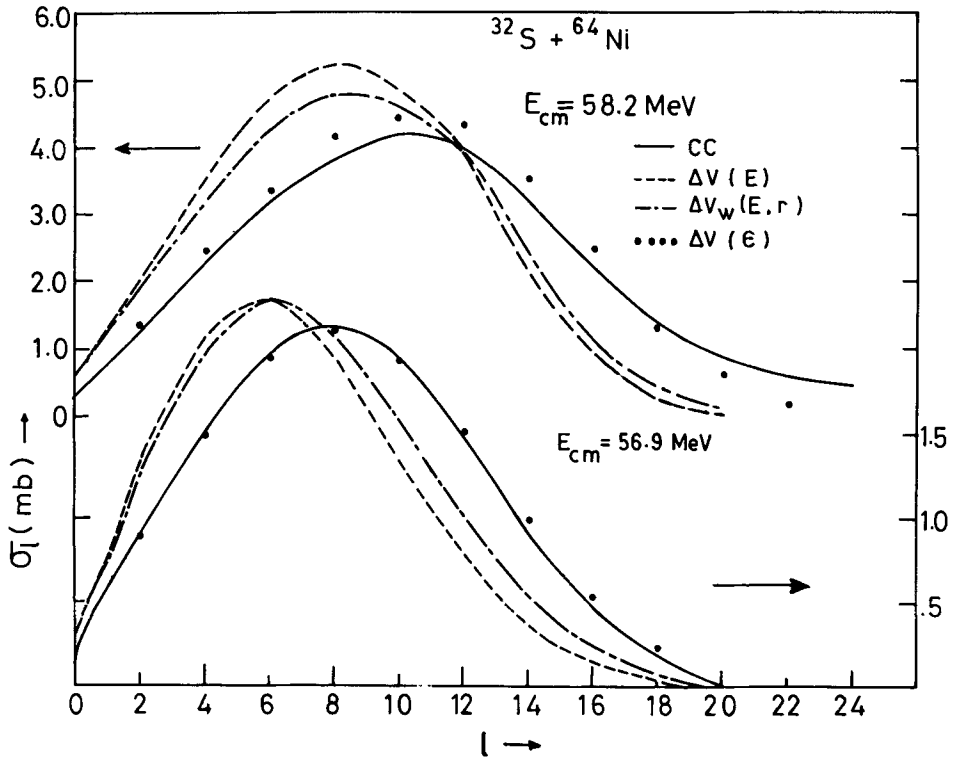

Figure 6. σ_l versus l at two different energies. The dashed curve and dashed-dot curve are the results with r-independent and r-dependent polarization potential $\Delta V(E)$ and $\Delta V_W(E,r)$. The solid curve is the result of the coupled channel calculation where the filled circles are results of BPM using ε-dependent polarization potential $\Delta V(\varepsilon)$.

with polarization potential ΔV which depends on ε (filled circle) is also shown in this figure. In this calculation, no explicit r-dependence was included. As seen from figure, the results of coupled channel calculation and results of ε-dependent ΔV are in good agreement. Inclusion of radial dependence in $\Delta V(\varepsilon)$ will make spin distribution still wider as in the case of $\Delta V(E)$.

4. Conclusion

It has been shown that, the barrier penetration model calculation including the proposed polarization potential ΔV are able to reproduce both fusion cross-section and spin distribution. The energy and radial dependent polarization potential $\Delta V(E,r)$ is not adequate to give rise to broad spin distribution even though it gives rise to correct fusion cross section. Although the radial dependence of polarization potential in optical model analysis give high spin distribution values (Satchler *et al* 1990; Satchler 1991 and Kubo *et al* 1991) such a high value is not reproduced with WKB penetration through real potential $V(r) + \Delta V(E,r)$. On the other hand, the present study shows that the barrier penetration through the real potential which depends on both energy and angular momentum gives rise to higher spin values. The polarization potential $\Delta V(\varepsilon)$ is calculated in a simple way from imaginary optical

potential using dispersion relation and is used in BPM model to explain experimental fusion and spin distributions.

Acknowledgement

We are thankful to Dr S S Kapoor and Dr V S Ramamurthy for many fruitful discussions.

References

Aguair C E, Canto L F, Donangelo R 1985 *Phys. Rev.* **C31** 1969
Baeza A, Bilwes B, Bilwes R, Diaz J and Ferrero J L 1984 *Nucl. Phys.* **A419** 412
Beckerman M 1985 *Phys. Rep.* **C129** 145
Beckerman M 1988 *Rep. Prog. Phys.* **51** 1047
Blocki J, Randrup J, Swiatecki W J and Tsang C F 1977 *Ann. Phys. (NY)* **105** 427
Broglia R A, Dasso C H, Landowne S L and Pollarollo G 1983 *Phys. Lett.* **B133** 34
Broglia R A, Dasso C H, Landowne S L and Pollarollo G 1985 *Phys. Lett.* **B133** 34
Dasgupta M, Navin A, Agarwal Y K, Baba C V K, Jain H C, Jhingan M L and Roy A 1991 *Phys. Rev. Lett.* **66** 1414
Dasgupta M, Navin A, Agarwal Y K, Baba C V K, Jain H C, Jhingan M L and Roy A 1992 *Nucl. Phys.* **A539** 351
Dasso C H and Landowne S 1987 *Comput. Phys. Commun.* **46** 187
Dasso C H, Landowne S and Pollaroio G 1989 *Phys. Lett.* **B217** 25
Dasso C H, Landowne S and Winther A 1983a *Nucl. Phys.* **A405** 381
Dasso C H, Landowne S and Winther A 1983b *Nucl. Phys.* **A407** 221
Esbensen H 1981 *Nucl. Phys.* **A352** 147
Fulton F R, Banes D W, Lilley J S, Nagarajan M A and Thompson I J 1985 *Phys. Lett.* **B162** 55
Halbert H L, Beene J R, Hensley D C, Honkanen K, Semkow T M, Abenante V, Sarantities D G and Li Z 1989 *Phys. Rev.* **C40** 2558
Iwamoto A and Harada K 1987 *Z. Phys.* **A326** 201
Kubo K I, Manyum P and Hodgson P E 1991 *Nucl. Phys.* **A534** 393
Lilley J S, Fulton B R, Nagarajan M A, Thompson I J and Banes D W 1985 *Phys. Lett.* **B151** 181
Mahaux C, Ngo H and Satchler G R 1986a *Nucl. Phys.* **A449** 354
Mahaux C, Ngo H and Satchler G R 1986b *Nucl. Phys.* **A456** 134
Mohanty A K, Sastry S V S, Kataria S K, Kailas S and Ramamurthy V S 1990 *Phys. Lett.* **B247** 215
Nagarajan M A, Mahaux C C and Satchler G R 1985 *Phys. Rev. Lett.* **54** 1136
Ramamurthy V S, Mohanty A K, Kataria S K and Rangarajan G 1990 *Phys. Rev.* **C41** 2702
Rhoades-Brown M J, Braun-Munzinger P 1984 *Phys. Lett.* **B136** 19
Satchler G R 1991 *Phys. Rep.* **199** 147
Satchler G R, Nagarajan M A, Lilley J S and Thompson I T 1990 *Phys. Rev.* **C41** 1869
Steadman S G (ed) 1985 *Fusion cross section below the coulomb barrier*, lecture notes in Physics V219 (Berlin: Springer)
Steadman S G and Rhoades-Brown M J 1986 *Ann. Rev. Nucl. Part. Sci* **36** 649
Stefanini A M *et al* 1987 *Phys. Rev. Lett.* **59** 2852
Udagawa T, Tamura T and Kim B T 1989 *Phys. Rev.* **C39** 1840
Vandenbosch R, Murakami T, Sahm C C, Leach D D, Ray A and Morphy M J 1986 *Phys. Rev. Lett.* **56** 1234
Wong C Y 1973 *Phys. Rev. Lett.* **31** 766